

Effects of nonlinearity on wave-packet dynamics in square and honeycomb lattices

W. S. Dias, M. L. Lyra, and F. A. B. F. de Moura

Instituto de Física, Universidade Federal de Alagoas, Maceió 57072-970, AL, Brazil

(Received 18 June 2010; revised manuscript received 10 September 2010; published 9 December 2010)

We offer a comparative study of the self-trapping phenomenon in square and honeycomb lattices, showing its dependence on the initial condition and lattice topology. In order to describe the dynamical behavior of one-electron wave packets, we use a discrete nonlinear Schrödinger equation which effectively takes into account the electron-phonon interaction in the limit of an adiabatic coupling. For narrow wave packets and strong nonlinearities, the electron distribution becomes trapped irrespective to the lattice geometry. In the opposite regime of wide wave packets and small nonlinearities, a delocalized regime takes place. There is an intermediate regime for which self-trapping is attained in the honeycomb lattice while the wave packet remains delocalized in square lattices. Further, we show that the critical nonlinear strength χ_c scales linearly with the initial wave-packet participation function $P(0)$ with the ratio $\chi_c/P(0)$ being on the order of the energy bandwidth.

DOI: [10.1103/PhysRevB.82.233102](https://doi.org/10.1103/PhysRevB.82.233102)

PACS number(s): 72.10.Di, 68.65.Pq, 72.80.Vp

I. INTRODUCTION

Within the context of fermions or bosons dynamics subjected to interaction with lattice vibrations, the effective description based on a discrete nonlinear Schrödinger equation (DNLSE) (Refs. 1–18) has attracted a wide interest. An effective cubic term in the time-dependent Schrödinger equation for the electron wave-packet dynamics arises after treating the phonon degrees of freedom within an adiabatic approximation which assumes that the local site polarization is much faster than the electron transfer between sites. The nonlinearity present in the DNLSE captures some essential features related to the electron-phonon dynamics,^{1–10} Bose-Einstein condensates (BECs),^{11,12} optical lattices,^{13,14} rogue waves,¹⁵ and coupled optical waveguides.^{16,17}

Within the electron-phonon dynamics context, the most important property associated with the DNLSE is the emergence of the so-called self-trapping phenomenon. In this case, an initially localized electronic wave packet remains localized in a finite region and there is a significant time-averaged probability to find the particle at the initial site. In Refs. 4 and 5, a very instructive amount of results about nonlinearity and electronic dynamics was reported. In particular, it was shown that either linear hosts with the presence of a nonlinear impurity or fully nonlinear lattices exhibit a self-trapping transition with universal features which are not affected by the lattice topology.⁵ Moreover, it was demonstrated that the DNLSE can display a wide class of topologically stable solutions such as solitons, vortex rings, and breathers (oscillatory solitonlike solutions).^{6–8} The standing or traveling nature of these solutions is associated to many properties of nonlinear discrete systems as, for example, energy transfer in biological chains.^{7,8} In fact, the presence of discrete solitons and breathers induced by nonlinearity has been intensive studied within the context of (BEC) (Ref. 9) waveguide arrays^{10,12} and general nonlinear systems.¹⁸

Recent experimental investigations using photoemission spectra have been widely used to investigate effects of electron-phonon interaction in pentacene films¹⁹ and graphene structures.²⁰ Graphene is a monolayer of carbon

atoms packed into a dense honeycomb crystal structure that can be viewed as an individual atomic plane extracted from graphite. Experimental developments have directed us closer to graphene-based nanoelectronics with components or even entire circuits formed from a graphene sheet. The graphene could allow electronic devices since it can be the best possible metal for metallic transistor applications.²¹ Following a description based on Dirac equations to graphene structures, the effects of electron-phonon interaction was studied.²² Within the cubic nonlinear Schrödinger equation context, the influence of the effective cubic nonlinearity arising from the adiabatic electron-phonon coupling in the electron dynamics was considered in two-dimensional lattices similar to graphene structures.^{23,24} In Ref. 23 the existence and stability of localized states in the discrete cubic nonlinear Schrödinger equation on two-dimensional nonsquare lattices was studied. The role played by nearest-neighbor as well as long-range interactions was pointed out in detail.²³ Furthermore, it was provided a systematic classification of the solutions that arise in hexagonal and honeycomb lattices with cubic nonlinearity.²⁴ The dynamics reveals the emergence of single-site solitary wave forms with a multisite breathing structure.²⁴

Motivated by the particular features of graphene,²² particularly its hexagonal geometry,²³ we offer a comparative study of the self-trapping phenomenon in square and honeycomb lattices, showing its dependence on the initial condition (initial width of wave packets). The self-trapping phenomenon is associated with the underlying interaction between electrons and lattice vibrations, responsible for a nonlinear contribution to the electronic Schrödinger equation. We will show that it takes stronger nonlinearities to promote self-trapping in square lattices than in honeycomb lattices and that the critical nonlinear strength scales linearly with the initial wave-packet distribution.

II. MODEL AND FORMALISM

In order to describe the dynamical behavior of an electron wave packet within a tight-binding approach, we used a dis-

crete nonlinear Schrödinger equation given by

$$i\hbar\dot{c}_{n,m}(t) = V \sum_{\langle n',m' \rangle} c_{n',m'}(t) - \chi |c_{n,m}(t)|^2 c_{n,m}(t), \quad (1)$$

where $c_{n,m}$ is the wave-packet amplitude at site (n,m) , V is the hopping amplitude between the nearest-neighbors sites $\langle n',m' \rangle$, and χ is a nonlinear parameter which is proportional to the local electron-phonon coupling.⁴ In what follows we will consider the particular cases of square and honeycomb geometries. Without any loss of generality, we are considering the on-site energies $\epsilon_{n,m}=0$ and will use units of $\hbar=V=1$.

To analyze the wave-packet propagation, we follow the time evolution of an initially Gaussian wave packet of width σ ,

$$c_{n,m}(0) = \frac{1}{A(\sigma)} \exp[-(n-n_0)^2/(4\sigma^2)] \times \exp[-(m-m_0)^2/(4\sigma^2)], \quad (2)$$

localized at site (n_0, m_0) . We employ the fourth-order Runge-Kutta method to numerically integrate Eq. (1). The electron will be considered to be initially located at the lattice center.

Aiming to characterize the dynamic behavior of the wave packet, we computed two typical quantities that can bring information about the possible self-trapping of the wave packet and its spacial extension, namely, the return probability and the participation function which are defined as

$$R(t) = |c_{n_0, m_0}(t)|^2 \quad (3)$$

and

$$P(t) = 1/\sum_{n,m} |c_{n,m}(t)|^4. \quad (4)$$

$R(t)$ gives the probability of finding the electron in the position corresponding to the center of the initial wave packet. Thus, $R(t \approx 10^6) \rightarrow 0$ means that the electronic wave function escapes from its initial location. Conversely, the return probability saturates at a finite value for a localized or a self-trapped wave packet. The participation function gives an estimate of the number of sites over which the wave packet is spread at time t . In the long-time regime, $P(t) \propto N^0$ indicates that the wave packet remains localized. On the other hand, $P(t) \propto N^2$ corresponds to the regime where the wave packet is distributed over the lattice.

III. SELF-TRAPPING IN HONEYCOMB AND SQUARE LATTICES

In Figs. 1(a) and 1(b), we show the time evolution of the participation function $P(t)$ computed for a wave packet with an initial Gaussian profile with participation function $P(t=0)=4$ spreading on (a) honeycomb and (b) square lattices with $N \times N = 1500 \times 1500$ sites and distinct strengths of the nonlinear parameter $\chi=25, 35$, and 50 . The wave-packet dynamics displays the same typical behavior for both lattices. For small values of χ , which represents a weak electron-phonon coupling, the wave packet extends continuously over

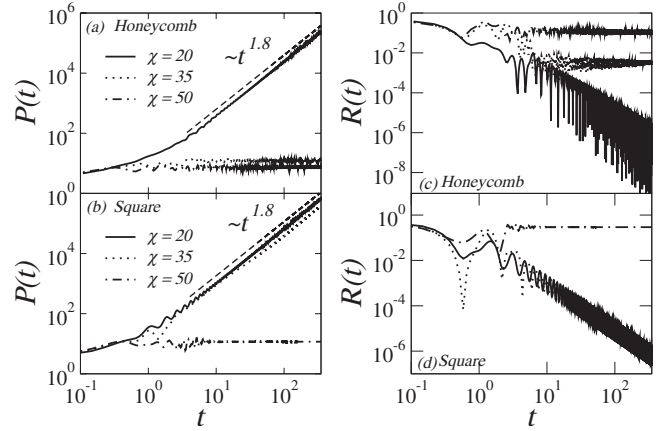


FIG. 1. Left panel: participation function $P(t)$ computed for lattices with $N \times N = 1500 \times 1500$ sites and different values of the nonlinear coupling $\chi=20, 35$, and 50 in (a) honeycomb and (b) square lattices. In all cases, the initial wave packet has a participation function $P(t=0)=4$. The reported data show the self-trapping of the wave packet as the strength of the electron-phonon coupling is increased. This feature is less pronounced in the square than in the honeycomb lattice. Right Panel: return probability $R(t)$ for the same values of lattice size, nonlinear couplings, and initial wave-packet extension in (c) honeycomb and (d) square lattices. The probability of return shows that, as we increase the nonlinear coupling, self-trapping occurs in the honeycomb lattice at smaller values of the nonlinearity than in the square lattice.

the entire lattice. For strong nonlinearities, the electron remains localized around its initial position. However, when comparing Figs. 1(a) and 1(b), we see that the electron is more susceptible to the electron-phonon coupling in the honeycomb than in the square lattice. Notice that the wave packet is extended in the square lattice and localized in the honeycomb lattice for the intermediate nonlinearity $\chi=35$. Such localization of the wave packet is the so-called self-trapping, on which the electron remains around its initial position due to its coupling with the lattice vibrations. In the delocalized regime, the growth of the participation function ultimately saturates for long runs as the wave packet reaches the lattice boundaries. This saturation is not reported in Fig. 1. In this case, the saturation value scales with the total number of lattice sites, in contrast with the size-independent value of the asymptotic participation function observed for self-trapped wave packets.

In order to better characterize the self-trapping phenomenon, we also report the time evolution of the return probability $R(t)$ for a wave packet with initial participation function $P(t=0)=4$ on the honeycomb lattice [Fig. 1(c)] and on the square lattice [Fig. 1(d)]. When the electron-phonon interaction is small, the electron becomes delocalized and the probability of finding it in the initial wave-packet position vanishes as t evolves. Conversely, the amplitude remains finite for a self-trapped wave packet, a phenomenon that takes place in the strong-coupling regime.

Data for the normalized participation function in the asymptotic regime $P(t \approx 10^6)/N^2$ versus the nonlinear parameter χ are shown in Fig. 2(a) for wave packets with an initial participation function of $P(t=0)=4$. In this case, the

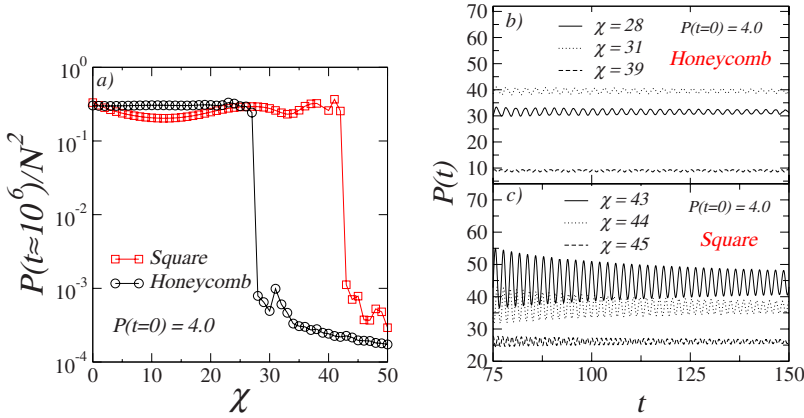


FIG. 2. (Color online) (a) Normalized asymptotic participation function $P(t \approx 10^6)/N^2$ versus the nonlinear coupling χ . An initial wave packet with $P(t=0)=4$ is considered. Notice a regime of intermediate nonlinearities for which self-trapping takes place in the honeycomb lattice while the wave packet remains delocalized in the square lattice. [(b) and (c)] The time evolution of the participation function in the vicinity of the self-trapping transition in (b) honeycomb and (c) square lattices. The oscillatory behavior is related to the breathing character of the self-trapped wave packets.

wave packet was allowed to spread until reaching a stationary state due to either reflections at the lattice boundaries or to self-trapping. A well defined self-trapping transition can be observed in both honeycomb and square lattices. In the delocalized phase, the participation function is on the order of the number of lattice sites. It exhibits a pronounced decrease at the critical nonlinearity strength above which the wave packet becomes trapped. These data show clearly that there is a range of nonlinear strengths for which self-trapping only takes place in the less connected honeycomb lattice. In addition, we show the time-dependent participation number versus time for wave packets with an initial participation function of $P(t=0)=4$ in both honeycomb and square lattices. Calculations were done considering nonlinearity degrees above the critical point. In Figs. 2(b) and 2(c), we show the time evolution of the participation function in the vicinity of the self-trapping transition. The oscillatory behavior reflects the breathinglike character of the self-trapped state.^{10,12,18,23} The oscillation amplitude decreases as one goes deeper into the self-trapped phase.

In order to quantify this comparative study of the self-trapping phenomenon in square and honeycomb lattices, we plot the phase diagram in the $P(t=0) \times \chi$ plane in Fig. 3. The extended states were characterized using the criterion $R(t \approx 10^6) \propto 1/N^2$ and $P(t \approx 10^6) \propto N^2$. The phase diagram depicts three main regions. The wave packet becomes delocalized in both square and honeycomb lattices for wide initial wave packets and small nonlinear strengths. In the opposite region of narrow initial wave packets and large nonlinear strengths, the wave-packet self-trapping predominates on both lattices. There is an intermediate stripe of the phase diagram in which self-trapping occurs in the less connected honeycomb lattice but not in the more connected square lattice. It is interesting to notice that the critical nonlinear strength on both lattices is proportional to the initial participation number and that the ratio $\chi_c/P(0)$ is on the order of the energy bandwidth. These results explicitly show the dependency of the self-trapping phenomenon on the initial condition (width of the wave packet) and that the local topology of the lattice is a relevant ingredient. In the inset of Fig. 3, we plot the critical nonlinearity strength normalized by the lattice coordination number. The curves from square and honeycomb lattices collapse showing that the lattice coordination is actually the relevant topological parameter influencing the self-trapping transition.

IV. SUMMARY AND CONCLUSIONS

In this work, we provided a detailed study of the one-electron wave-packet self-trapping transition in square and honeycomb lattices. Self-trapping results from a nonlinear contribution to the Schrödinger time-dependent equation for the wave-packet dynamics that arises from the adiabatic coupling of the moving electron with the underlying lattice vibrations. For strong nonlinear couplings, the effective on-site potential around which the electron is initially placed becomes well above the energy band. This leads to a decoupling of this energy level and, consequently, to the wave-packet trapping. We provided a comparative study of the self-trapping transition in typical two-dimensional lattices in order to characterize the influence of the lattice topology, as well as the influence of the initial wave-packet profile. We showed that in the less connected honeycomb lattice, a smaller nonlinear strength is required to promote self-

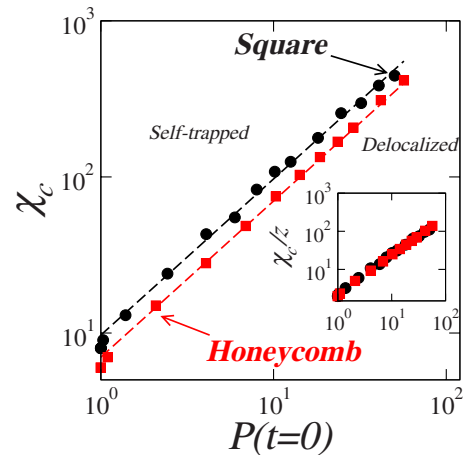


FIG. 3. (Color online) Phase diagram in the $P(t=0) \times \chi$ parameter space showing the transition from the delocalized to the self-trapped phase. The regime of delocalized wave packets was characterized using the criterion $R(t \approx 10^6) \propto 1/N^2$ and $P(t \approx 10^6) \propto N^2$. It takes stronger nonlinearities to promote self-trapping in square lattices than in honeycomb lattices. In both cases, the critical nonlinearity scales linearly with the initial participation function. In the inset, we report the critical nonlinearity normalized by the lattice coordination number. The collapse of the curves indicates that the lattice coordination is the relevant topological parameter for the self-trapping transition.

trapping. This feature is directly related to the fact that the honeycomb lattice depicts a narrower energy band when compared to the more connected square lattice. Therefore, the lattice coordination is the relevant topological parameter controlling the self-trapping transition. Further, we showed that the critical nonlinear strength scales linearly with the participation function of the initial wave packet. For both lattices, the ratio between the critical nonlinear strength and the initial participation function is on the order of the energy bandwidth. Therefore, the self-trapping localization transition is strongly influenced by both lattice topology and wave-

packet initial distribution. It would be interesting to extend the present scenario to more general models incorporating electron-electron interactions, disorder, and nonlinearity, in order to settle the relative role played by Mott, Anderson and self-trapping localization in distinct lattice topologies.

ACKNOWLEDGMENTS

This work was partially supported by CNPq, CAPES, and FINEP (Federal Brazilian Agencies), CNPq-Rede Nanobioestruturas, as well as FAPEAL (Alagoas State Agencies).

-
- ¹G. Kopidakis, S. Komineas, S. Flach, and S. Aubry, *Phys. Rev. Lett.* **100**, 084103 (2008); A. S. Pikovsky and D. L. Shepelyansky, *ibid.* **100**, 094101 (2008); D. Hajnal and R. Schilling, *ibid.* **101**, 124101 (2008); S. Flach, D. O. Krimer, and Ch. Skokos, *ibid.* **102**, 024101 (2009); Ch. Skokos, D. O. Krimer, S. Komineas, and S. Flach, *Phys. Rev. E* **79**, 056211 (2009).
- ²F. A. B. F. de Moura, I. Gléria, I. F. dos Santos, and M. L. Lyra, *Phys. Rev. Lett.* **103**, 096401 (2009); F. A. B. F. de Moura, E. J. G. G. Vidal, I. Gléria, and M. L. Lyra, *Phys. Lett. A* **374**, 4152 (2010).
- ³V. M. Kenkre and D. K. Campbell, *Phys. Rev. B* **34**, 4959 (1986); V. M. Kenkre and H.-L. Wu, *ibid.* **39**, 6907 (1989); P. Grigolini, H.-L. Wu, and V. M. Kenkre, *ibid.* **40**, 7045 (1989).
- ⁴D. Chen, M. I. Molina, and G. P. Tsironis, *J. Phys.: Condens. Matter* **5**, 8689 (1993); **8**, 6917 (1996); C. A. Bustamante and M. I. Molina, *Phys. Rev. B* **62**, 15287 (2000); M. I. Molina, *ibid.* **58**, 12547 (1998).
- ⁵M. I. Molina, *Phys. Rev. B* **60**, 2276 (1999); G. P. Tsironis, M. I. Molina, and D. Hennig, *Phys. Rev. E* **50**, 2365 (1994); M. I. Molina, *Mod. Phys. Lett. B* **13**, 837 (1999).
- ⁶E. Arévalo, *Phys. Rev. Lett.* **102**, 224102 (2009); M. Öster and M. Johansson, *Phys. Rev. E* **73**, 066608 (2006).
- ⁷O. Braun and Yu. S. Kivshar, *Phys. Rep.* **306**, 1 (1998).
- ⁸D. Hennig and G. P. Tsironis, *Phys. Rep.* **307**, 333 (1999).
- ⁹A. Trombettoni and A. Smerzi, *Phys. Rev. Lett.* **86**, 2353 (2001).
- ¹⁰J. W. Fleischer, T. Carmon, M. Segev, N. K. Efremidis, and D. N. Christodoulides, *Phys. Rev. Lett.* **90**, 023902 (2003).
- ¹¹B. B. Wang, P. M. Fu, J. Liu, and B. Wu, *Phys. Rev. A* **74**, 063610 (2006).
- ¹²J.-K. Xue and A.-X. Zhang, *Phys. Rev. Lett.* **101**, 180401 (2008).
- ¹³N. Akhmediev, A. Ankiewicz, and J. M. Soto-Crespo, *Phys. Rev. E* **80**, 026601 (2009).
- ¹⁴S. A. Ponomarenko and G. P. Agrawal, *Phys. Rev. Lett.* **97**, 013901 (2006).
- ¹⁵A. Maluckov, Lj. Hadzievski, N. Lazarides, and G. P. Tsironis, *Phys. Rev. E* **79**, 025601(R) (2009).
- ¹⁶Y. Lahini, A. Avidan, F. Pozzi, M. Sorel, R. Morandotti, D. N. Christodoulides, and Y. Silberberg, *Phys. Rev. Lett.* **100**, 013906 (2008).
- ¹⁷Th. Anker, M. Albiez, R. Gati, S. Hunsmann, B. Eiermann, A. Trombettoni, and M. K. Oberthaler, *Phys. Rev. Lett.* **94**, 020403 (2005).
- ¹⁸N. K. Efremidis and K. Hizanidis, *Phys. Rev. Lett.* **101**, 143903 (2008); J. Cuevas, L. Q. English, P. G. Kevrekidis, and M. Anderson, *ibid.* **102**, 224101 (2009); G. Assanto, L. A. Cisneros, A. A. Minzoni, B. D. Skuse, N. F. Smyth, and A. L. Worthy, *ibid.* **104**, 053903 (2010); R. A. Vicencio and S. Flach, *Phys. Rev. E* **79**, 016217 (2009).
- ¹⁹R. C. Hatch, D. L. Huber, and H. Höchst, *Phys. Rev. Lett.* **104**, 047601 (2010).
- ²⁰M. Bianchi, E. D. L. Rienks, S. Lizzit, A. Baraldi, R. Balog, L. Hornekaer, and Ph. Hofmann, *Phys. Rev. B* **81**, 041403 (2010); A. Grüneis, C. Attaccalite, A. Rubio, D. V. Vyalikh, S. L. Molodtsov, J. Fink, R. Follath, W. Eberhardt, B. Büchner, and T. Pichler, *ibid.* **79**, 205106 (2009).
- ²¹K. S. Novoselov, A. K. Geim, S. V. Morozov, D. Jiang, Y. Zhang, S. V. Dubonos, I. V. Grigorieva, and A. A. Firsov, *Science* **306**, 666 (2004).
- ²²A. H. Castro Neto, F. Guinea, N. M. Pere, K. S. Novoselov, and A. K. Geim, *Rev. Mod. Phys.* **81**, 109 (2009).
- ²³P. G. Kevrekidis, B. A. Malomed, and Yu. B. Gaididei, *Phys. Rev. E* **66**, 016609 (2002).
- ²⁴K. J. H. Law, P. G. Kevrekidis, V. Koukouloyannis, I. Kourakis, D. J. Frantzeskakis, and A. R. Bishop, *Phys. Rev. E* **78**, 066610 (2008).